

# Resonance nucleon scattering amplitude in the photonuclear reaction

Swapan Das

*Nuclear Physics Division, Bhabha Atomic Research Centre,  
Trombay, Mumbai 400085, India*

*Homi Bhabha National Institute, Anushakti Nagar, Mumbai 400094, India*

## Abstract

The cross section of the photonuclear reaction in the nucleon-resonance region is calculated to search the resonance-nucleon scattering amplitude in the nucleus. It is assumed that the resonance  $R$  is produced and decayed in the elementary photon-nucleon ( $\gamma N$ ) reaction in the nucleus as  $\gamma N \rightarrow R \rightarrow \gamma N$ . The resonance interacts with the nucleons while propagating through the nucleus. Therefore, the calculated photonuclear reaction cross section is compared with the data to extract the resonance-nucleon scattering parameters in the nucleus.

## 1 Introduction

The photonuclear reaction is a pertinent probe to investigate various aspects of basic research and application in physics, see Ref. [1] for review. This reaction is a key ingredient to investigate the nucleosynthesis in the universe. The photonuclear reaction triggered by the lighting discharge [2] has been used to observe the previously unknown channels for generating carbon, nitrogen and oxygen isotopes. Since the photon induced nuclear reaction does not create distortion in the entrance channel, it is a potential tool to study the final state interactions of the produced hadrons [3]. The nuclear transparency measured for the photoproduced  $\omega$  and  $\phi$  mesons illustrates the  $\omega N$  and  $\phi N$  cross sections in the nucleus are larger than the respective cross sections in the free space [4]. The photonuclear reaction is in extensive use to explore the color transparency of hadrons [5] (also see the references therein).

The remarkable observation in the measured energy distribution spectrum of the photonuclear reaction in the resonance region ( $\approx 0.2 - 1.2$  GeV) [6, 7] is the disappearance of certain resonances which are distinctly visible in that measured for the photonucleon reaction [8, 9, 10]. The spectra measured for nuclei show the  $\Delta(1232)$ -peak is partially modified whereas the peaks of higher resonances (e.g.,  $N(1520)$ , ..... ) are vanished in the nucleus. The change in the spectral-shape of resonances in a nucleus occurs because of the nuclear medium effect on them. The Fermi-motion of the nucleon in a nucleus produces the suppression and broadening of the resonance peak. The resonance-nucleus interaction can also dampen and widen the peak of the resonance, which is addressed as the collision

broadening of the resonance. It linearly depends on the in-medium resonance-nucleon cross section, i.e.,  $\Gamma_R^c \propto \sigma_t^{*RN}$  [11].

The photonuclear reaction in the resonance region has been studied by Rapp et al., [12] using the vector-meson dominance model which states the photon is converted to the transverse  $\rho$ -meson. Hence, the  $\gamma$ -nucleon resonances have been interpreted as the  $\rho$ -nucleon resonances. The parameters appearing in this calculation are extracted by fitting the calculated photoproton reaction cross section with the data. Using those parameters, the cross section of the photonuclear reaction is evaluated. The Fermi-motion of the nucleon in the nucleus is not considered in the calculation. The nuclear effect is evaluated by the Lindhard function describing the resonance dynamics in the nucleus. The calculated results are shown in well accord with the data reported for nuclei [12]. Kondratyuk et al., [13] have also calculated the cross section of the photonuclear reaction in the quoted energy region by evaluating the forward Compton scattering amplitude of the reaction. They have extracted the  $\gamma$ -nucleon resonances' parameters (i.e., mass and width) by fitting the calculated photonucleon reaction cross sections with the data, and used those to evaluate the cross section of the photonuclear reaction. The effect of the Fermi-motion of the nucleon is estimated by the Fermi-suppression factor. The resonance-nucleus interaction is described by the optical potential generated by folding the resonance-nucleon scattering amplitude with the nuclear density. The resonance-nucleon cross section in the nucleus is extracted from the measured cross section of the photonuclear reaction.

The cross sections of the photonuclear reaction is also calculated in this paper. The Fermi-suppression factor evaluated by Kondratyuk et al., [13], as mentioned above, is used to assess the effect of the Fermi-motion of the bound nucleon. The optical potential for the resonance-nucleus interaction is also formulated by folding the resonance-nucleon scattering amplitude with the nuclear density. The forward Compton scattering amplitude of both the photonucleon and photonuclear reactions (used to calculate the cross section) differs from that done by Kondratyuk et al., [13] in the following ways. The measured mass and width of all four-starred resonances [8] (except those of the  $\Delta(1232)$  resonance) are used in the calculation. The photon-nucleon interactions are described by the Lagrangians, which are used to evaluate the spin-isospin matrix elements associated with the production and decay of the resonances. The calculated cross sections of the photonucleon reactions are fitted with the data to extract the resonance-nucleon-photon coupling-constants appearing in the Lagrangians. The propagator of the resonance is taken as the eikonal form in the Glauber model [11], which illustrates the propagation of the resonance from the production point to the decay point in the nucleus. The calculated results of the photonuclear reaction are fitted with the measured cross sections [6] to extract the resonance-nucleon scattering amplitude (not only the cross section) in the nucleus.

## 2 Formalism

The Lagrangian describing the resonance  $R$  production due to the nucleon-photon  $N\gamma$  coupling is categorized based on the positive or negative parity state of  $R$ . For the positive parity state, the Lagrangian describing the  $RN\gamma$  coupling is given by [12, 14]

$$\mathcal{L}_{RN\gamma} = \frac{f_{RN\gamma}}{m_\pi} R^\dagger (\mathbf{s}^\dagger \times \mathbf{k}_\gamma) \cdot \epsilon(\lambda_\gamma) i_r^\dagger N. \quad (1)$$

The spin operator  $\mathbf{s}^\dagger = \sigma(\mathbf{S}^\dagger)$  connects  $N$  of  $J^P = \frac{1}{2}^+$  to  $R$  of  $J^P = \frac{1}{2}^+(\frac{3}{2}^+)$ , where  $J^P$  denotes spin<sup>parity</sup> of the particle.  $i_r^\dagger = \tau_r(I_r^\dagger)$  does the isospin  $\frac{1}{2} \rightarrow \frac{1}{2}(\frac{3}{2})$  transition of the particle.

For  $R$  of  $J^P = \frac{5}{2}^+$ , the Lagrangian is expressed by Friman et al., [15] as

$$\mathcal{L}_{RN\gamma} = \frac{f_{RN\gamma}}{m_\pi} R^\dagger S_{ij}^\dagger k_{\gamma,i} \epsilon_j i_r^\dagger N, \quad (2)$$

where  $S_{ij}^\dagger$  denotes the spin  $\frac{1}{2}^+ \rightarrow \frac{5}{2}^+$  transition operator. It is a tensor of rank 2 and  $6 \times 2$  matrix in spin space. The spin transition matrix [15] is

$$\langle R | S_{ij}^\dagger k_{\gamma,i} \epsilon_j | N \rangle = \langle X_{ij} | k_{\gamma,i} \epsilon_j | N \rangle. \quad (3)$$

$|X_{ij}\rangle$  can be constructed by coupling of two spin-1 objects  $\epsilon_i^s$  to the nucleon spinor  $\chi_{1/2}^{m_s}$  [15], i.e.,

$$|X_{ij}^M\rangle = \sum_{r,s,t,m_s} C(2r \frac{1}{2} m_s | \frac{5}{2} M) C(1s1t | 2r) \epsilon_i^s \epsilon_j^t | \chi_{1/2}^{m_s} \rangle, \quad (4)$$

where the unit vectors are given by

$$\epsilon^{+1} = -\frac{1}{2}(1, i, 0), \quad \epsilon^0 = (0, 0, 1), \quad \text{and} \quad \epsilon^{-1} = \frac{1}{2}(1, -i, 0). \quad (5)$$

The evaluation of the matrix element for spin- $\frac{5}{2}$  object has been discussed elaborately in Ref. [15].

The Lagrangian describing the transition  $N$  of  $J^P = \frac{1}{2}^+$  to  $R$  of  $J^P = \frac{1}{2}^-(\frac{3}{2}^-)$  is given by [12, 14]

$$\mathcal{L}_{RN\gamma} = \frac{f_{RN\gamma}}{m_\pi} R^\dagger (E_\gamma \mathbf{s}^\dagger \cdot \epsilon(\lambda_\gamma) - \epsilon^0(\lambda_\gamma) \mathbf{s}^\dagger \cdot \mathbf{k}_\gamma) i_r^\dagger N, \quad (6)$$

where  $\epsilon^0$  (the time-component of photon polarization) is zero for the real photon, as it has only transverse polarizations [16]. The coupling constants  $f_{R\gamma N}$  appearing in the Lagrangians  $\mathcal{L}_{RN\gamma}$  are discussed later.

The nucleus  $A$  is assumed as a composition of the nucleon  $N$  and nucleus  $B$ . The photon  $\gamma$  couples to  $N$  and produces the resonance  $R$  which (after propagating certain distance) decays to  $N'\gamma'$ . The nucleon  $N'$  recombines with  $B$  to form the nucleus  $A'$  in the final state. Symbolically, it can be represented as  $\gamma A \rightarrow RB \rightarrow \gamma' A'$ . The  $T$ -matrix of the reaction can be written as

$$T_{fi}^{\gamma A} = \int \int d\mathbf{r}' d\mathbf{r} \sum_{R,B} \langle \gamma' A' | \Gamma_{RN\gamma}^\dagger | RB \rangle G_R(\mathbf{r}' - \mathbf{r}) \langle BR | \Gamma_{RN\gamma} | \gamma A \rangle, \quad (7)$$

where  $\Gamma_{RN\gamma}$  denotes the vertex operator. It can be expressed by the Lagrangians in Eqs. (1), (2) and (6) without the wave-functions of the nucleon and resonance included in it.

$G_R(\mathbf{r}' - \mathbf{r})$  in Eq. (7) represents the propagation of the resonance  $R$  from the production (space) coordinate  $\mathbf{r}$  to the decay coordinate  $\mathbf{r}'$ . Since the forward  $T$ -matrix is related the cross section of the reaction, the eikonal approximation in the Glauber model is used to expressed  $G_R(\mathbf{r}' - \mathbf{r})$  [11]:

$$G_R(\mathbf{r}' - \mathbf{r}) = \delta(\mathbf{b}' - \mathbf{b}) \theta(z' - z) e^{i\mathbf{k}_R \cdot (\mathbf{r}' - \mathbf{r})} D_{\mathbf{k}_R}(\mathbf{b}, z', z), \quad (8)$$

where  $\mathbf{b}(\mathbf{b}')$  is the impact factor for  $\mathbf{r}(\mathbf{r}')$  in the cylindrical coordinate system. The non-relativistic form of  $D_{\mathbf{k}_R}(\mathbf{b}, z', z)$  is given by

$$D_{\mathbf{k}_R}(\mathbf{b}, z', z) = -\frac{i}{v_{R\parallel}} \exp \left[ \frac{i}{v_{R\parallel}} \int_z^{z'} dz'' \{ \Delta(m) - V_{OR}(\mathbf{b}, z'') \} \right] \quad (9)$$

with  $\Delta(m) = m - m_R + \frac{i}{2}\Gamma_R$ .  $m$  is the invariant mass of the decay-products (i.e.,  $N\gamma$  in the considered reaction) of the resonance  $R$ .  $m_R$  and  $\Gamma_R$  are the resonant mass and width of  $R$ , as listed in table-1.  $V_{OR}$  denotes the resonance-nucleus optical potential elaborated later.  $v_{R\parallel}$  is the velocity of the resonance ( $v_R$ ) parallel to the beam direction.

After taking the average over the initial state and the summation over the final state, the  $T$ -matrix for the elastic photon scattering on a spin zero nucleus can be written as  $\bar{T}_{ii}^{\gamma A} = \frac{1}{2} \sum_{\lambda_\gamma \lambda_{\gamma'}} T_{ii}^{\gamma A}$ , where  $\lambda_\gamma(\lambda_{\gamma'})$  denotes the polarization of the incoming (outgoing) photon. The Compton scattering amplitude  $F_{ii}^{\gamma A}$  is related to  $\bar{T}_{ii}^{\gamma A}$  as  $F_{ii}^{\gamma A} = \frac{m_A}{4\pi\sqrt{s}} \bar{T}_{ii}^{\gamma A}$  [17], where  $m_A$  is the mass of the target and  $\sqrt{s}$  denotes the total energy in the center of mass system. In the considered energy region (i.e.,  $\leq 1.2$  GeV), the above equation can be reduced to  $F_{ii}^{\gamma A} \approx \frac{1}{4\pi} \bar{T}_{ii}^{\gamma A}$  for a nucleus [17]. The total scattering cross section  $\sigma_t^{\gamma A}(R)$  of the photonuclear reaction due to the resonance  $R$  is

$$\sigma_t^{\gamma A}(R) = \frac{4\pi}{k_\gamma} \text{Im}[F_{ii}^{\gamma A}]. \quad (10)$$

Table 1: Four-starred resonances  $R$  taken from Ref. [8].  $J^P$  denotes  $spin^{parity}$  of  $R$ .  $m_R$  and  $\Gamma_R$  are the mass and width respectively of  $R$  used in the calculation. The range of the measured  $m_R$  and  $\Gamma_R$  are given in the bracket.

$J^P$	$R$	$m_R(\text{MeV})$	$\Gamma_R(\text{MeV})$
$\frac{1}{2}^+$	$N(1440)$	1440 (1410-1470)	350 (250-450)
	$N(1710)$	1710 (1680-1740)	140 (80-200)
	$\Delta(1910)$	1910 (1850-1950)	300 (200-400)
$\frac{3}{2}^+$	$\Delta(1232)$	1220 (1230-1234)	110 (114-120)
	$\Delta(1600)$	1600 (1500-1640)	250 (200-300)
	$N(1720)$	1720 (1680-1750)	250 (150-400)
	$N(1900)$	1900 (1890-1950)	200 (100-320)
$\frac{5}{2}^+$	$N(1680)$	1680 (1680-1690)	120 (115-130)
	$\Delta(1905)$	1905 (1855-1910)	330 (270-400)
$\frac{1}{2}^-$	$N(1535)$	1535 (1515-1545)	150 (125-175)
	$\Delta(1620)$	1620 (1590-1630)	130 (110-150)
	$N(1650)$	1650 (1635-1665)	125 (100-150)
	$N(1895)$	1895 (1870-1920)	120 (80-200)
$\frac{3}{2}^-$	$N(1520)$	1510 (1510-1520)	110 (100-120)
	$\Delta(1700)$	1700 (1690-1730)	300 (220-380)

The above formalism can be modified to calculate the cross section  $\sigma_t^{\gamma N}$  of the photonucleon reaction (i.e.,  $\gamma N \rightarrow R \rightarrow \gamma' N'$ ), where the Fermi-motion of the nucleon and the resonance-nucleus potential do not exist. The  $T$ -matrix for this reaction can be written as

$$T_{ii}^{\gamma N} = \int \int d\mathbf{r}' d\mathbf{r} \sum_R \langle \gamma' N' | \Gamma_{RN\gamma}^\dagger | R \rangle G_R(\mathbf{r}' - \mathbf{r}) \langle R | \Gamma_{RN\gamma} | \gamma N \rangle. \quad (11)$$

$V_{OR}$  appearing in  $G_R(\mathbf{r}' - \mathbf{r})$ , see Eqs. (9) and (8), is equal to zero for the photonucleon reaction. To evaluate  $\sigma_t^{\gamma N}$ , the polarizations of the photons and the spins of the nucleons in the initial and final states have to be accounted for taking the average over the initial state and the summation over the final state.

### 3 Results and Discussion

The cross sections of the photonucleon and photonuclear reactions have been calculated in the resonance region, i.e.,  $E_\gamma \approx 0.2 - 1.2$  GeV. The background contributions to the cross

sections are taken from Ref. [13]. The resonance-nucleon-photon coupling-constants  $f_{RN\gamma}$  in the calculated cross sections of the photonucleon reactions are adjusted so that the calculated results added with the background of the reactions reproduce the data. Those values of  $f_{RN\gamma}$  are used to evaluate the cross sections of the photonuclear reactions.

The calculated total cross sections of the photoproton  $\gamma p$  reaction are presented in Fig. 1, where  $\sigma_t^{RN}(R)$  represents the cross section of the  $\gamma p$  reaction occurring because of the individual resonance  $R$ . The short-long-short-dashed curve [labeled as  $\Sigma_R \sigma_t^{RN}(R)$ ] in Fig. 1(a) denotes the calculated cross section due to all resonances, as listed in table-1. The long-dashed curve (labeled as  $BG$ ) refers to the background of the reaction [13]. The dot-dashed curve (labeled as  $\Sigma_R \sigma_t^{RN}(R) + BG$ ) in Fig. 1(a) arising due to the addition of the calculated results (short-long-short-dashed curve) and the background (long-dashed curve) is compared with the measured cross section of the  $\gamma p$  reaction [8, 9]. The extracted values of the resonance-proton-photon coupling-constants  $f_{Rp\gamma}$  are listed in table-2. The short-long-short-dashed curve in Fig. 1(b) is already explained in Fig. 1(a). The dominant contributions to the cross section of the  $\gamma p$  reaction, as represented by the short-dashed curves [labeled as  $\sigma_t^{RN}(R)$ ] in Fig. 1(b), arise due to the  $\Delta(1232)$ ,  $N(1520)$ , and  $N(1680)$  resonances. Amongst them, the cross section because of the  $\Delta(1232)$  resonance is distinctly largest. The cross sections of the above reaction due to other resonances are not shown explicitly, as their contributions to the cross section are less significant.

The total cross sections of the photoneutron  $\gamma n$  reaction have been shown in Fig. 2. The curves appearing in this figure represent the  $\gamma n$  reaction cross sections similar to those explained in Fig. 1 for the  $\gamma p$  reaction, except the cross section due to the  $N(1680)$  resonance in the  $\gamma n$  reaction is insignificant [could not be shown Fig. 2(b)] in contrast to that occurring in the  $\gamma p$  reaction [see Fig. 1(b)]. The resonance-neutron-photon coupling-constants  $f_{Rn\gamma}$  in the calculated cross section of the  $\gamma n$  reaction, as shown in Fig. 2(a), have been determined using the data taken from Ref. [10]. The values of  $f_{Rn\gamma}$  are also listed in table-2.

The cross sections of the photonuclear reactions have been calculated for nuclei, where the nuclear effect, i.e., the Fermi-motion of the bound nucleon and the resonance-nucleus interaction, are investigated. The Fermi-motion causes the suppression and broadening of the cross section. To describe it, the Fermi-suppression factor estimated by Kondratyuk et al., (as shown in Fig. 3 in Ref. [13]) has been incorporated in the calculation. The interaction of the resonance with the nucleus is addressed by the resonance-nucleus optical potential  $V_{OR}$ , which is generated by folding the forward resonance-nucleon scattering amplitude  $f_{RN}$  (in the free space) with the density of nucleus [18], i.e.,

$$-\frac{1}{v_R} V_{OR}(\mathbf{r}) = \frac{2\pi}{k_R} f_{RN}(0) \varrho(\mathbf{r}) = \frac{1}{2} [\alpha_{RN} + i] \sigma_t^{RN} \varrho(\mathbf{r}). \quad (12)$$

$\varrho(\mathbf{r})$  denotes the spatial distribution of the nuclear density, as extracted from the electron

Table 2: The resonance-nucleon-photon coupling constants  $f_{RN\gamma}$  appearing in the Lagrangians in Eqs. (1), (2) and (6), as extracted from the measured cross sections of the photonucleon reactions.

$\frac{1}{2}^+$	$f_{p(1440)p\gamma} = 1.28 \times 10^{-2}$	$f_{n(1440)n\gamma} = 1.68 \times 10^{-2}$
	$f_{p(1710)p\gamma} = 1.22 \times 10^{-3}$	$f_{n(1710)n\gamma} = 1.22 \times 10^{-3}$
	$f_{\Delta^+(1910)p\gamma} = 3.85 \times 10^{-3}$	$f_{\Delta^0(1910)n\gamma} = 3.85 \times 10^{-3}$
$\frac{3}{2}^+$	$f_{\Delta^+(1232)p\gamma} = 0.114$	$f_{\Delta^0(1232)n\gamma} = 0.102$
	$f_{\Delta^+(1600)\gamma p} = 2.86 \times 10^{-3}$	$f_{\Delta^0(1600)\gamma n} = 2.86 \times 10^{-3}$
	$f_{p(1720)\gamma p} = 6.21 \times 10^{-3}$	$f_{n(1720)\gamma n} = 3.92 \times 10^{-3}$
	$f_{p(1900)\gamma p} = 1.42 \times 10^{-3}$	$f_{n(1900)\gamma n} = 1.8 \times 10^{-3}$
$\frac{5}{2}^+$	$f_{p(1680)\gamma p} = 3.21 \times 10^{-2}$	$f_{n(1680)\gamma n} = 6.42 \times 10^{-3}$
	$f_{\Delta^+(1905)\gamma p} = 2.44 \times 10^{-2}$	$f_{\Delta^0(1905)\gamma n} = 1.57 \times 10^{-2}$
$\frac{1}{2}^-$	$f_{p(1535)\gamma p} = 8.27 \times 10^{-3}$	$f_{n(1535)\gamma n} = 3.7 \times 10^{-3}$
	$f_{\Delta^+(1620)p\gamma} = 6.33 \times 10^{-3}$	$f_{\Delta^0(1620)n\gamma} = 6.33 \times 10^{-3}$
	$f_{p(1650)p\gamma} = 5.59 \times 10^{-3}$	$f_{n(1650)n\gamma} = 1.25 \times 10^{-3}$
	$f_{p(1895)p\gamma} = 2.02 \times 10^{-3}$	$f_{n(1895)n\gamma} = 1.11 \times 10^{-3}$
$\frac{3}{2}^-$	$f_{p(1520)p\gamma} = 3.2 \times 10^{-2}$	$f_{n(1520)n\gamma} = 2.57 \times 10^{-2}$
	$f_{\Delta^+(1700)p\gamma} = 1.48 \times 10^{-2}$	$f_{\Delta^0(1700)n\gamma} = 6.05 \times 10^{-3}$

scattering data [19]. In fact, the electron scattering determines the proton density of the nucleus. Therefore,  $\varrho(\mathbf{r})$  is approximated by the proton density with the normalization:  $4\pi \int r^2 \varrho(r) dr = A$  (mass number of the nucleus).  $\alpha_{RN}$  represents the ratio of the real to imaginary parts of  $f_{RN}$ .  $\sigma_t^{RN}$  is the total resonance-nucleon scattering cross section:  $\sigma_t^{RN} = \frac{4\pi}{k_R} \text{Im}[f_{RN}]$ . The above form of the optical potential of the hadron is largely used to study the nuclear reactions [20]. These quantities in the nucleus (symbolized by  $\alpha_{RN}^*$  and  $\sigma_t^{*RN}$ ), as done later, have been extracted by fitting the calculated photonuclear cross section with that of the measured value.  $V_{OR}$  with  $\alpha_{RN}^*$  and  $\sigma_t^{*RN}$  defines the resonance-nucleus potential in the reaction. Since  $V_{OR}$  is absorptive, the peak cross section of the reaction due to the resonance  $R$  is attenuated by the factor  $\frac{\sigma_t^{\gamma A(R)} V_{OR} \neq 0}{\sigma_t^{\gamma A(R)} V_{OR} = 0}$  because of the inclusion of the potential in the calculation.

The cross section per nucleon  $\sigma_t^{\gamma C}/A$  of the photcarbon  $\gamma C$  reaction is calculated without considering the Fermi-motion of the bound nucleon and the resonance-nucleus interaction [i.e., potential  $V_{OR}$  in Eq. (12)]. The resonance-nucleon-photon coupling-constants  $f_{RN\gamma}$  extracted from the photonucleon reactions, as listed in table-2, are used in the calculation. The calculated results versus the beam energy  $E_\gamma$  are presented in Fig. 3.

The short-dashed and the short-long-short curves appearing in the figure qualitatively illustrate those explained in Fig. 1(b) for the  $\gamma p$  reaction, i.e., the dominant contributions to the cross section of the  $\gamma C$  reaction arise due to the  $\Delta(1232)$ ,  $N(1520)$  and  $N(1680)$  resonances.

The photonuclear cross section  $\sigma_t^{\gamma C}/A$  due to all resonances for the carbon nucleus is evaluated including the Fermi-motion of the bound nucleon and the resonance-nucleus optical potential in the calculation. The Fermi-motion, as mentioned earlier, is addressed by the Fermi-suppression factor [13]. In Fig. 4, the calculated cross sections  $\sigma_t^{\gamma C}/A$  is represented by the dot-dot-dashed curve and the background of the reaction (as given in Ref. [13]) is denoted by the long-dashed curve. The calculated results added with the background, as represented by the solid curve, are fitted with the data [6] to extract the resonance-nucleon scattering parameters [i.e.,  $\alpha_{RN}^*$  and  $\sigma_t^{*RN}$  as described in Eq. (12)] in the nucleus. As shown in Fig. 3, the  $\Delta(1232)$ ,  $N(1520)$  and  $N(1680)$  resonances contribute dominantly to the cross section. Therefore,  $\alpha_{RN}^*$  and  $\sigma_t^{*RN}$  for these resonances are quoted in table-3.

Table 3: The scattering parameters, i.e.,  $\alpha_{RN}^*$  and  $\sigma_t^{*RN}$ , of the  $\Delta(1232)$ ,  $N(1520)$  and  $N(1680)$  resonances in the nucleus.  $\sigma_t^{*RN}$  estimated by Kondratyuk et al., [13] is also compared.

$R$	$\alpha_{RN}^*$	$\sigma_t^{*RN}$ (mb)	$\sigma_t^{*RN}$ (mb) in Ref. [13]
$\Delta(1232)$	1.34	54.11	78.94
$N(1520)$	0.57	426.25	183.36
$N(1680)$	-0.31	425.33	153.06

The sensitivities of the Fermi-motion ( $FM$ ) of the bound nucleon and the resonance-nucleus potential ( $V_{OR}$ ) to the calculated cross section  $\sigma_t^{\gamma C}/A$  (without the background contribution) are exhibited in Fig. 5.  $V_{OR}$  is estimated using the extracted values of  $\alpha_{RN}^*$  and  $\sigma_t^{*RN}$  for the resonances. The short-long-short-dashed curve (also shown in Fig. 3) represents  $\sigma_t^{\gamma C}/A$  of the  $\gamma C$  reaction, where  $FM$  and  $V_{OR}$  are not considered in the calculation. The medium-dashed curve results because of the inclusion of the Fermi-suppression factor due to the Fermi-motion [13], as described earlier, in the calculated cross section. The suppression and broadening of the resonance peaks due to the Fermi-motion is distinctly visible in Fig. 5. In fact, the peaks in the region of  $N(1520)$  and  $\Delta(1700)$  resonances are smeared out significantly due to the Fermi-motion. The dot-dot-dashed curve (also appeared in Fig. 4) denotes the calculated  $\sigma_t^{\gamma C}/A$  due to both  $FM$  and  $V_{OR}$  incorporated in the calculation.

The cross section of the photoinduced reaction on the  $^{208}\text{Pb}$  nucleus has been eval-



uated using the Fermi-motion of the bound nucleon (as done for the  $^{12}\text{C}$  nucleus) and the resonance-nucleus interaction potential  $V_{OR}$  in the calculation. The values of the in-medium scattering parameters (i.e.,  $\alpha_{RN}^*$  and  $\sigma_t^{*RN}$ ) extracted from the photocarbon reaction, as discussed earlier, are used to determine  $V_{OR}$ . The calculated results (denoted by the solid curve) are compared with the data [6] in Fig. 6(a). The average of the cross sections assessed for  $^{12}\text{C}$  and  $^{208}\text{Pb}$  nuclei, as shown by the solid curve in Fig. 6(b), agrees with the measured average cross section of the photonuclear reactions [6].

## 4 Conclusions

The cross section of the photonuclear reaction has been calculated to explore the scattering parameters of the resonances in the nucleus. The calculated results for the  $^{12}\text{C}$  nucleus are fitted with the data to extract the in-medium scattering parameters of the resonances. Using those parameters, the cross section of the photolead reaction is evaluated and compared that with the data. The average measured cross section of the photonuclear reactions is reproduced well by that of the calculated results.

## 5 Acknowledgement

The author thanks A. K. Gupta and S. M. Yusuf for their encouragement to work on the theoretical nuclear physics.

## References

- [1] A. Zilges, D. L. Balabanski, J. Isaak, and N. Pietralla, *Prog. Part. Nucl. Phys.* **122** (2022) 103903.
- [2] T. Enoto, Y. Wada, Y. Furuta, K. Nakazawa, T. Yuasa et al., *Nature* **551** (2017) 481.
- [3] V. E. Tarasov, W. J. Briscoe, H. Gao, A. E. Kudryavtsev and I.I. Strakovsky, *Phys. Rev. C* **84** (2011) 035203; K. Gottfried and D. I. Julius, *Phys. Rev. D* **1** (1970) 140; A. Pautz and G. Shaw, *Phys. Rev. C* **57** (1988) 2648.
- [4] S. Das, *Eur. Phys. J. A* **55** (2019) 186; P. Mühlich and U. Mosel, *Nucl. Phys. A* **773** (2006) 156; P. Mühlich, V. Shklyar, S. Leupold, U. Mosel, and M. Post, *ibid.* **780** (2006) 187; T. Ishikawa et al., *Phys. Lett. B* **608** (2005) 215.

- [5] D. Dutta, K. Hafidi and M. Strikman, *Prog. Part. Nucl. Phys.* **69** (2013) 1; S. Das, *Phys. Rev. C* **105** (2022) 035204; *ibid.* **107** (2023) 035201.
- [6] N. Bianchi, V. Muccifora, E. De Sanctis, A. Fantoni, P. Lavi Sandri et al., *Phys. Rev. C* **54** (1996) 1688.
- [7] V. Muccifora, N. Bianchi, A. Deepman, E. De Sanctis, M. Mirazita et al., *Phys. Rev. C* **60** (1999) 064616; M. Anghinolfi, V. Lucherini, P. Rossi, N. Bianchi, P. Corvisiero et al., *Phys. Rev. C* **47** (1993) R922; N. Bianchi et al. *Phys. Lett. B* **299** (1993) 219; **309** (1993) 5; **325** (1994) 333; Th. Frommhold, F. Steiper, W. Henkel, U. Kneissl, J. Ahrens et al., *Z. Phys. A* **350** (1994) 249; J. Ahrens, *Nucl. Phys. A* **446** (1985) 229c.
- [8] P. A. Zyla et al., (Particle Data Group), *Prog. Theor. Exp.* **2020** (2020) 083C01; <https://pdg.lbl.gov/2020/hadronic-xsections>.
- [9] T. A. Armstrong, W. R. Hogg, G. M. Lewis, A. W. Robertson et al., *Phys. Lett. B* **34** (1971) 535; *Phys. Rev. D* **5** (1972) 1640.
- [10] T. A. Armstrong, W. R. Hogg, G. M. Lewis, A. W. Robertson et al., *Nucl. Phys. B* **41** (1972) 445.
- [11] S. Das, *Phys. Rev. C* **103** (2021) 035205.
- [12] R. Rapp, M. Urban, M. Buballa and J. Wambach, *Phys. Lett. B* **417** (1998) 1.
- [13] L. A. Kondratyuk, M. I. Krivoruchenko, N. Bianchi, E. De Sanctis, and V. Muccifora, *Nucl. Phys. A* **579** (1994) 453.
- [14] W. Peters, M. Post, H. Lenske, S. Leupold and U. Mosel, *Nucl. Phys. A* **632** (1998) 109.
- [15] B. Friman and H. J. Pirner, *Nucl. Phys. A* **617** (1997) 496.
- [16] F. Halzen and A. D. Martin, *Quarks and Leptos*, (John Wiley & Sons, New York, 1984) p. 134.
- [17] T. Ericson and W. Weise, *Pions and Nuclei*, (Clarendon Press, Oxford, 1988) page nos. 23 and 431.
- [18] R. J. Glauber, in *Lectures in Theoretical Physics*, edited by W. E. Brittin et al. (Interscience, New York, 1959), Vol. I, p. 315; J. M. Eisenberg and D. S. Kolton, *Theory of Meson Interaction with Nuclei* (John Wiley & Sons, New York, 1980) p. 158.

- [19] C. W. De Jager, H. De Vries and C. De Vries, *At. Data and Nucl. Data Tables* **14** (1974) 479; H. De Vries, C. W. De Jager and C. De Vries, *ibid.* **36** (1987) 495.
- [20] L. Frankfurt, M. Strikman and M. Zhalov, *Phys. Rev. C* **67** (2003) 034901; T. Falter, S. Leupold and U. Mosel, *Phys. Rev. C* **62** (2000) 031602(R); S. Das, *Phys. Rev. C* **100** (2019) 035203; *Phys. Scr.* **96** (2021) 035304.

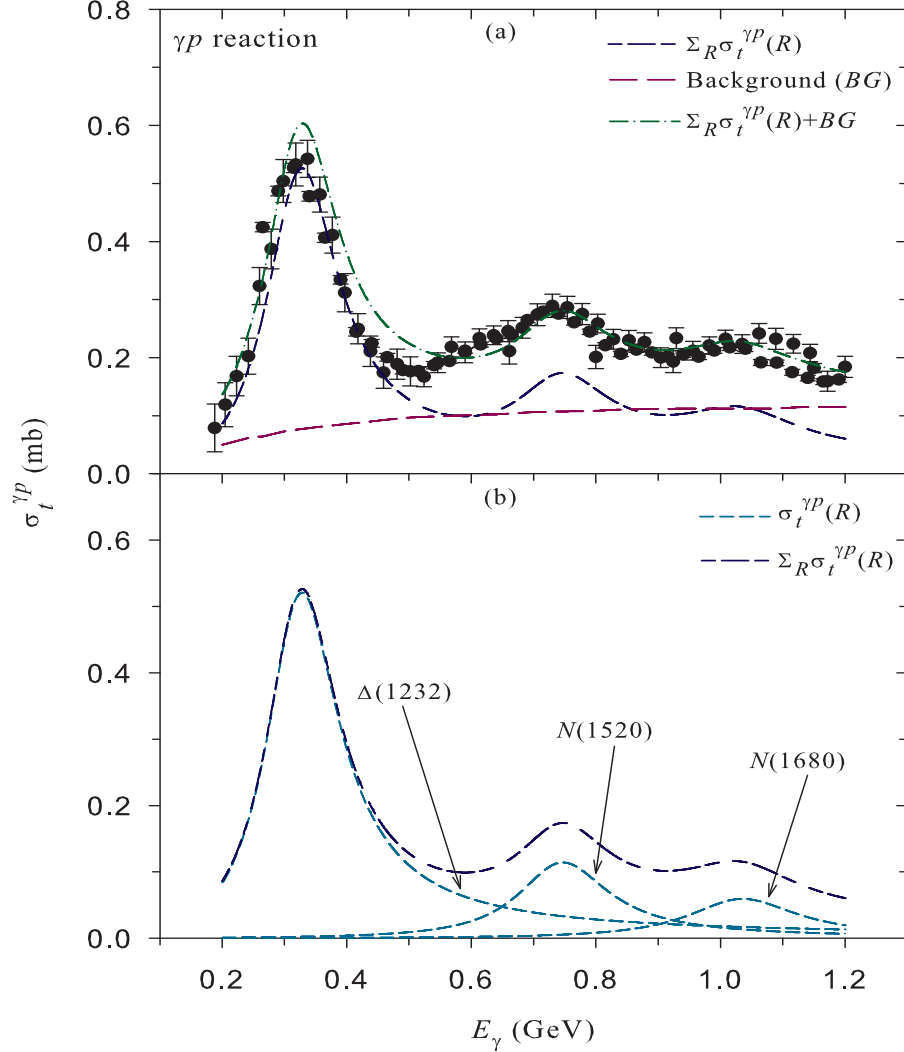


Figure 1: (color online). Upper part (a): The calculated total cross section  $\sigma_t^{\gamma p}$  of the photoproton  $\gamma p$  reaction. The short-long-short-dashed curve occurs due to the contributions of all resonances, as listed in table 1, to the calculated cross section. The long-dashed curve represents the background contribution to the cross section [13]. The dot-dashed curve arises due to the addition of the above curves. The data are taken from Refs. [8, 9]. Lower part (b): The short-dashed curves represent the cross sections due to the  $\Delta(1232)$ ,  $N(1520)$  and  $N(1680)$  resonances. The short-long-short curve is already described in the upper part (a) of the figure.

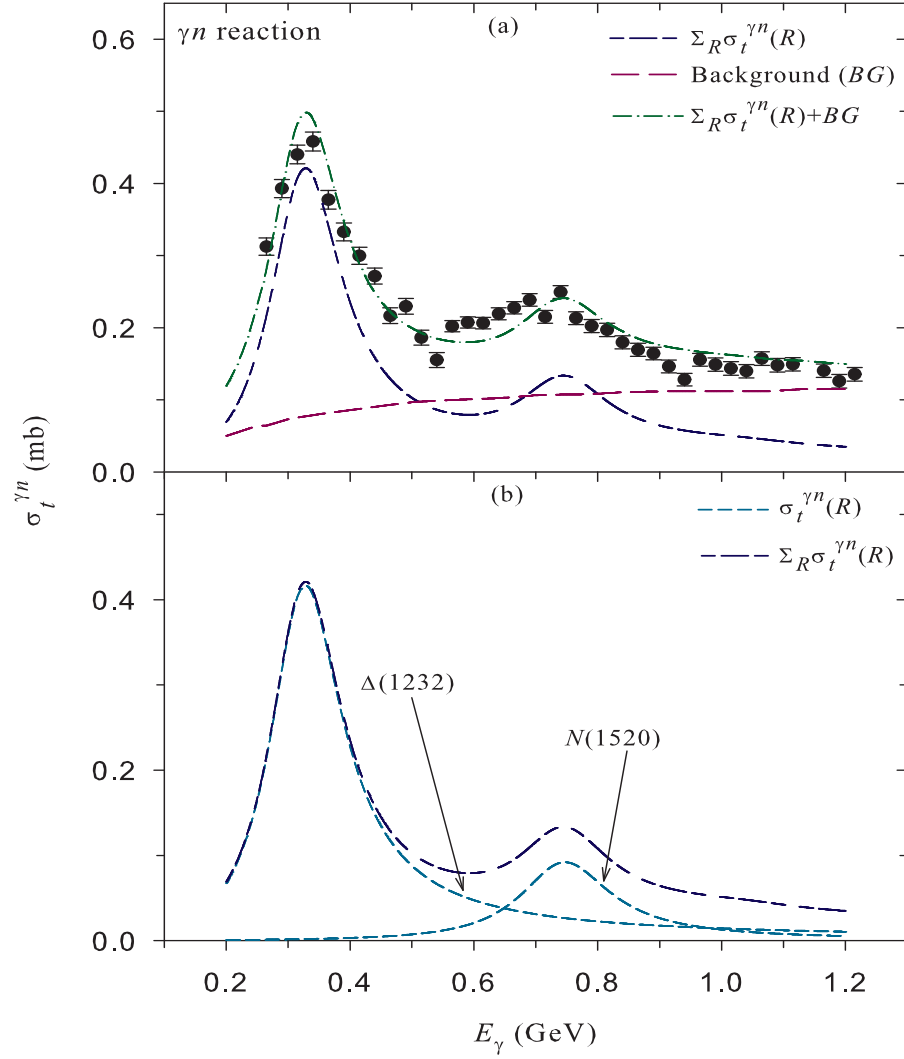


Figure 2: (color online). As in Fig. 1 but for the photoneutron  $\gamma n$  reaction, see text. The data are taken from Ref. [10].

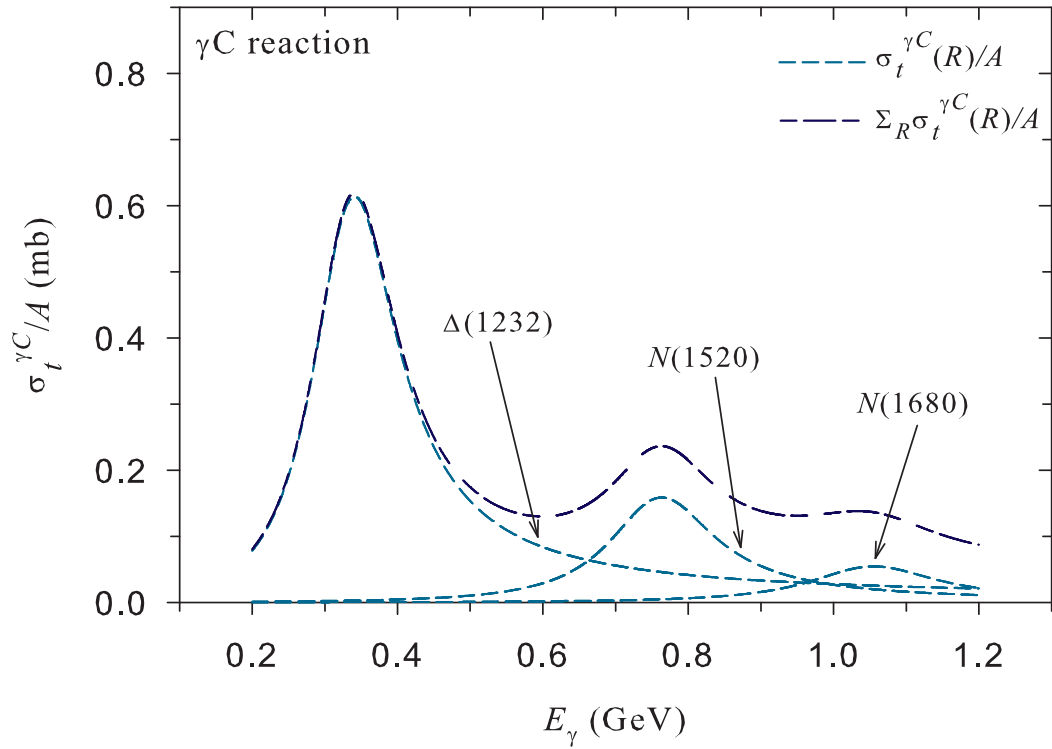


Figure 3: (color online). Total cross section per nucleon  $\sigma_t^{\gamma C}/A$  of the photoreaction  $\gamma C$  calculated without considering the Fermi-motion and the resonance-nucleus interaction. The curves appearing in the figure qualitatively represent those explained in Fig. 1(b).

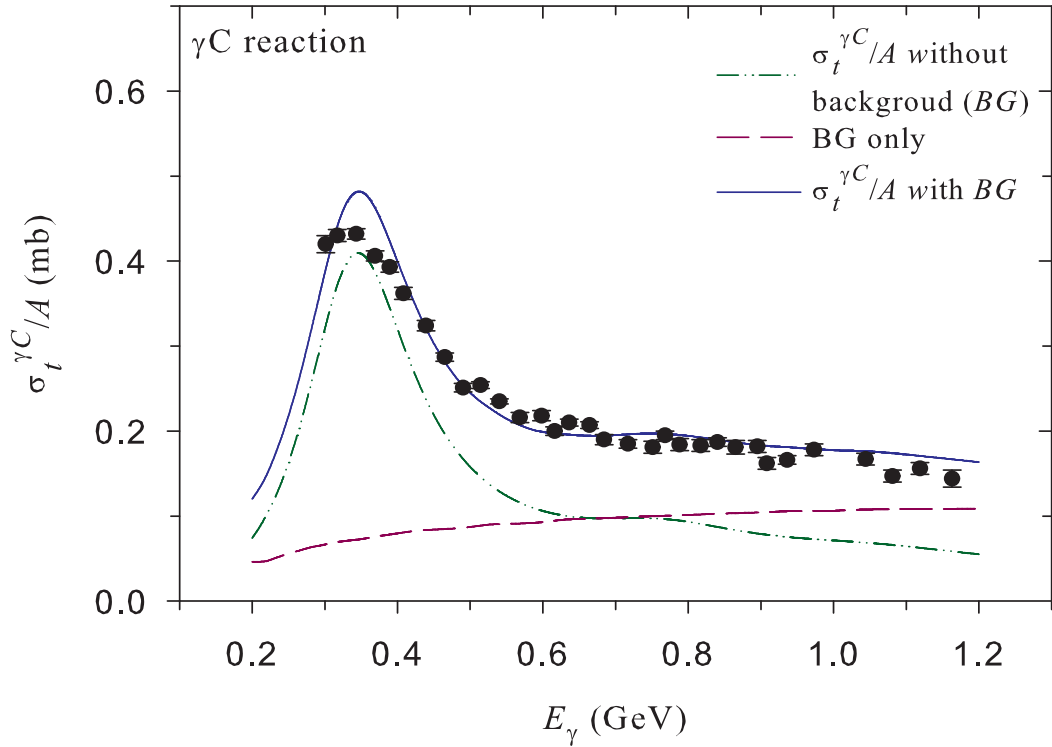


Figure 4: (color online). The cross section/nucleon  $\sigma_t^{\gamma C}/A$  due to all resonances calculated using the Fermi-motion of the bound nucleon, and the resonance-nucleus interaction potential is represented by the dot-dot-dashed curve. The long-dashed curve is the background contribution to the cross section [13]. The solid curve arises because of the summation of the above curves. See text for the detail. The data are taken from Ref. [6].

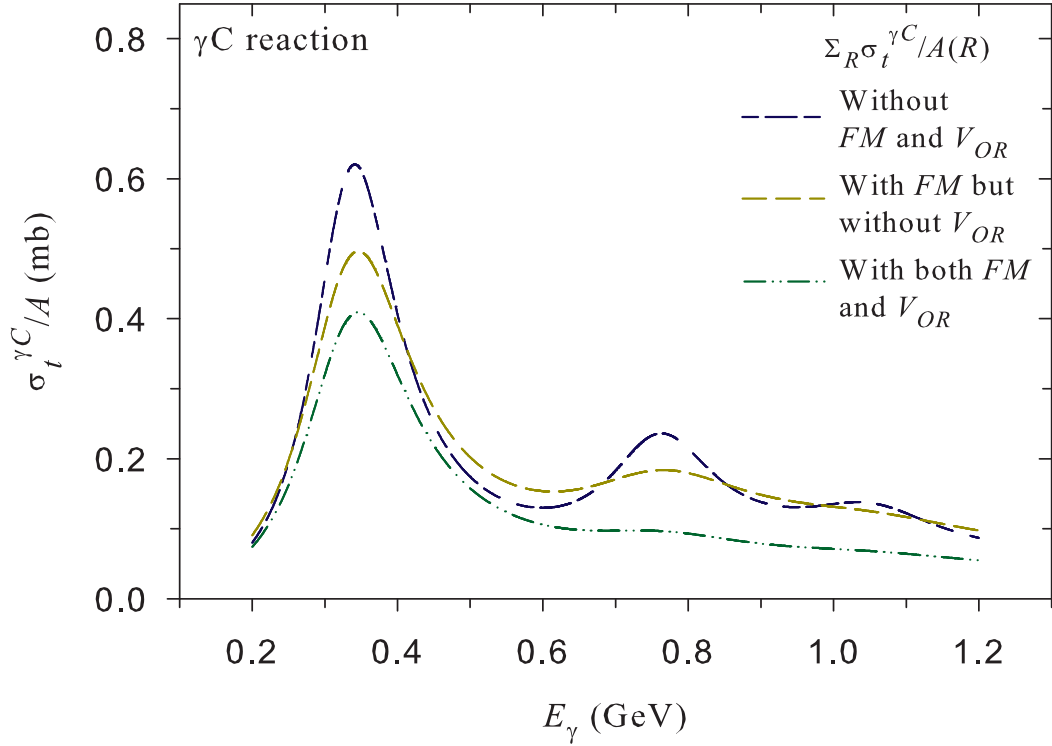


Figure 5: (color online). The short-long-short-dashed curve represents the calculated total cross section per nucleon  $\sigma_t^{\gamma C}/A$  due to all resonances, as done in Fig. 3. The medium-dashed curve denotes  $\sigma_t^{\gamma C}/A$  evaluated incorporating the Fermi-motion ( $FM$ ) of the bound nucleon, whereas the dot-dot-dashed curve (also shown in Fig. 4) represents that assessed including both  $FM$  and the resonance-nucleus optical potential  $V_{OR}$  in the calculation.



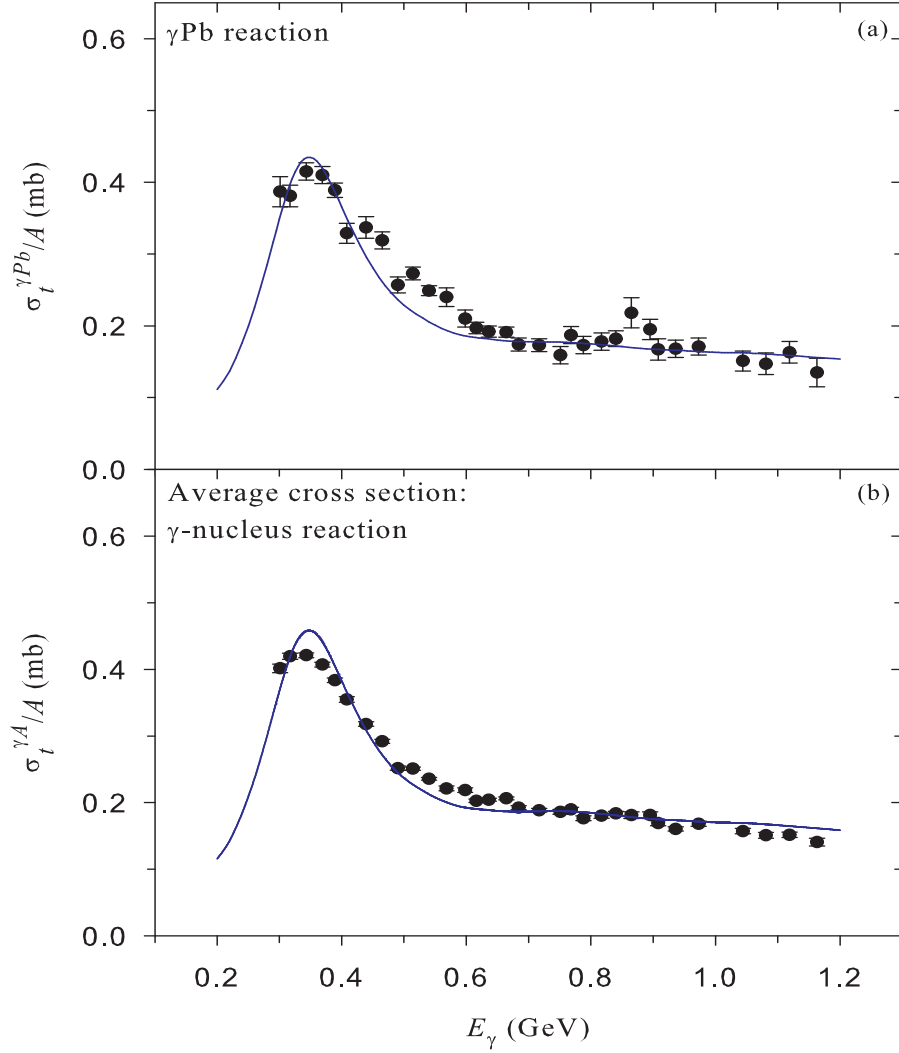


Figure 6: (color online). Upper part (a): The solid curve represent that in Fig. 4 but for  $^{208}\text{Pb}$  nucleus. Lower part (b): The average of the cross sections calculated for  $^{12}\text{C}$  and  $^{208}\text{Pb}$  nuclei (denoted by the solid curve) is compared with the measured value. The data appearing in the figure are taken from Ref. [6].